# Mixtures of Ionic Liquids and Sulfolane as Electrolytes for Li-Ion Batteries

Andreas Hofmann,[1,*] Michael Schulz,[1] Sylvio Indris,[2] Ralf Heinzmann,[2,3] Thomas Hanemann[1,4]

1) Karlsruher Institut für Technologie (KIT), Institut für Angewandte Materialien - Werkstoffprozesstechnik, Hermann-von-Helmholtz-Platz 1, 76344 Eggenstein-Leopoldshafen, Germany

2) Karlsruher Institut für Technologie (KIT), Institut für Angewandte Materialien - Energiespeichersysteme, Hermann-von-Helmholtz-Platz 1, 76344 Eggenstein-Leopoldshafen, Germany

3) Bruker Biospin GmbH, Silberstreifen 4, 76287 Rheinstetten, Germany.

4) Universität Freiburg, Institut für Mikrosystemtechnik, Georges-Köhler-Allee 102, 79110 Freiburg, Germany

* Corresponding Author:

Andreas Hofmann

Karlsruher Institut für Technologie (KIT), Institut für Angewandte Materialien - Werkstoffprozesstechnik (IAM-WPT), Hermann-von-Helmholtz-Platz 1, 76344 Eggenstein-Leopoldshafen, Germany

Telephone: +49 (0)721-608-25920; Fax: +49 (0)721-608-22095; e-mail: andreas.hofmann2@kit.edu

## Abstract

In this study, novel temperature stable electrolyte mixtures are investigated with respect to their use in Li-ion cells. Sulfolane, 3-methylsulfolane, and the ionic liquid N,N-diethyl-N-methyl-N-(2-methoxyethyl)ammonium bis(trifluoromethanesulfonyl)azanide (DMMA-TFSA) are chosen as main components in the electrolyte mixtures. The electrolytes are investigated in cell tests with $LiNi_{1/3}Mn_{1/3}Co_{1/3}O_2$ (NMC) as cathode and graphite as anode material. The performance of the cells is tested at room temperature and at elevated temperatures (40 °C) which demonstrates the significant improvement of the cell performance by raising the temperature slightly. Furthermore, the additives vinylene carbonate and hexamethyldisilazane are used to improve the electrolyte properties with respect to cell performance and long term stability.

**Keywords:** electrolytes; Li-ion battery; organic solvents; ionic liquids;

## Introduction

Lithium-ion batteries are the most prospective chemical energy storage tools for high power electrical applications like the automotive sector. However, there are still challenges regarding safety (flammability), high voltage, and toxicity issues for Li-ion cells. Therefore, alternative electrolyte mixtures are besides the electrode investigation still one of the main focus areas of the battery researchers.

Up to date, most commercial electrolytes are mixtures based on organic carbonates and $LiPF_6$. Namely, dimethyl carbonate (DMC), diethyl carbonate (DEC), and ethylmethyl carbonate (EMC) are used extensively in spite of their high flammability. Therefore, the battery has to be prepared with different kinds of safety tools which reduce the risk of fire or explosion, but increase the cost of the cell pack. Thus, electrolyte mixtures should be developed which enable an improvement in the intrinsic cell safety.

One interesting class of electrolyte solvents regarding high voltage applications and high safety are sulfolane derivatives [1-4]. An outstanding electrochemical oxidation stability, a moderate conductivity, an appropriate dipole moment and dielectric constant, a high flash point and boiling point, and the stability of aluminum against dissolution at high potentials are main advantages [5-8] of these class of compounds. As expected, the anion of the lithium salt contributes and affects the physicochemical and electrochemical properties of such sulfolane – conducting salt mixtures significantly [5]. However, the cell performance is considerably reduced compared to carbonate-based mixtures because of the increased viscosity [8]. Furthermore, additives are mentioned to be necessary to obtain an accurate solid electrolyte interface (SEI) film onto negative graphite electrodes [8, 9]. Sedlarikova et al. demonstrated the principal use of sulfolane (SL) and mixtures of sulfolane (SL) with carbonates (DMC, propylene carbonate (PC)) and the conducting salt $LiClO_4$ in Li-ion based cells [6]. However,

a fast fading was observed against graphite anodes [6]. Li et al. proved mixtures of SL and sulfites with lithium bis(oxalato)borate (LiBOB) as conducting salt to be an option as electrolyte solvents for Li-ion cells [10], but the addition of these compounds reduce the flash points significantly.

Another approach to enhance the safety of the battery cell is the use of ionic liquids (IL) as electrolyte component or additive because of the negligible vapor pressure and high flash points (> 300 °C) [11-13]. It is found that N,N-diethyl-N-methyl-N-(2-methoxyethyl)ammonium bis(trifluoromethylsulfonyl)azanide (DMMA-TFSA) effectively hampers the aluminum dissolution at high voltages against $Li/Li^+$ [14] and provides an acceptable ionic conductivity [15, 16] which makes it very attractive as electrolyte component. In addition, the replacement of the conducting salt $LiPF_6$ with more temperature stable salts like LiBOB or lithium bis(trifluoromethanesulfonyl)azanide (LiTFSA) increases the safety properties, too [17, 18]. However, there are still challenges based on the long term stability of such electrolyte mixtures because of aluminum dissolution at high cell voltages, solid electrolyte interface (SEI) stability and capacity fading [19].

Very recently, Xiang et al. published the usability of mixtures of sulfolane and ionic liquid (piperidinium based IL) as electrolytes for Li-ion half cells ($Li/LiFePO_4$ and $Li/Li_{1.2}Ni_{0.2}Mn_{0.6}O_2$) for up to 50 cycles [20]. However, lithium cannot be used in commercial cells because of the growth of Li dendrites onto the surface of Li. Furthermore, a quasi-infinite reservoir of Li impedes the analysis of the cell regarding lithium fading, solid electrolyte interface (SEI) stability, long-time stability, and continuous consumption of Li for the SEI layer.

The aim of this study is to evaluate the feasibility of novel sulfolane (SL) and DMMA-TFSA mixtures including the sulfolane derivative 3-methylsulfolane (M-SL) as electrolyte component in Li-ion based batteries against graphite. Therefore, the electrolytes are studied in the cell system graphite and $LiNi_{1/3}Mn_{1/3}Co_{1/3}O_2$. In addition, the effects of selected additives

are investigated, namely vinylene carbonate (VC), hexamethyldisilazane (HMDS), and lithium bis(oxalato)borate (LiBOB), which are necessary to obtain a stable SEI layer and preferably reduced capacity fading.

## Experimental

N,N-diethyl-N-methyl-N-(2-methoxyethyl)ammonium bis(trifluoromethylsulfonyl)azanide (DMMA-TFSA, IoLiTec, > 99.8%), lithium bis(trifluoromethylsulfonyl)azanide (LiTFSA, IoLiTec, > 99.5%), sulfolane (SL, Sigma-Aldrich, 99%), and 3-methylsulfolane (M-SL, TCI europe, >98%, 725 ppm $H_2O$) were dried at 120°C (Karl-Fischer). Vinylene carbonate (VC, Aldrich, 97%), hexamethyldisilazane (HMDS, Sigma-Aldrich, 99%), lithium bis(oxalato)borate (Chemetall), lithium foil (Alfa Aesar, 0.75 mm thick), and aluminum foil (Hohsen Corp., Japan, current collector quality) were used as received. The preparation of the electrolytes was performed in an argon-filled glove box (MBraun GmbH) with oxygen and water levels below 0.5 ppm. During the preparation of the electrolyte mixtures which vary in their HMDS content (E-9, E-10, E-11, E-12), it is observed that the glass vial is silanized for very high concentrations (8 m.-%) and that the solubility limit is nearly reached. Calandered electrodes based on graphite and NMC with a content of approximately 90% of active material were provided in cooperation.

For the drying procedure and the verification of the water content, a coulombmetric Karl-Fischer titratior was used. The titrator consists of a 831 KF Coulometer and a 860 KF Thermoprep oven from Metrohm. The water content of the solvents was less than 10 ppm.

In this study common coin cells (type: CR 2032, Hohsen Corp.) were used with a coin cell crimper from BT Innovations (Canada). The cells were assembled in an argon-filled glove box according to standard procedures. Precisely, a graphite anode (Ø = 15 mm), a NMC cathode (Ø = 15 cm), and a glass fiber separator (Whatman®, GF/B and QMA 450; Ø =16

mm) were used inside a coin type cell with one spring and one stainless steel spacer (electrolyte volume: 140 µl).

The ionic conductivity of the electrolytes was measured by the standard complex impedance method, using a Zahner Zennium IM6 electrochemical workstation in the frequency range from 1 kHz to 1 MHz. A 1.6 ml closed cell (0.85 ml solvent) from RHD instruments is used for the measurements. The temperature dependence (0 – 80 °C) of the ionic conductivity was recorded by placing the test cells in a temperature and humidity chamber (ThermoTec Espec, SH-261). Before each measurement the cells were thermally equilibrated for at least 30 min. In the phase minimum (~ 0°) the impedance value $|\vec{Z}|$ was used for calculating the specific conductivity κ according to $\kappa = C/|\vec{Z}|$ with the cell constant C = 17.0139 $cm^{-1}$. The cell constant was received by measuring a standard solution (1.413 mS $cm^{-1}$ at 25 °C, Hanna instruments, HI 70031). The internal resistance of the cells were measured via complex impedance. The value of the resistance, which is mentioned in the text, was extracted from the Bode-plot in the minimum of the phase (~ 0°).

The cyclovoltamogramms were measured at a Zahner XPOT potentiostat (software: PPSeries, Potentiostat XPot Zahner elektrik 6.4). The potential range was 2.5 – 6 V vs. $Li/Li^+$ with platinum as working electrode. The cells were measured in 3-electrode configuration (EE-Cells manufactured by EL-Cell GmbH) with reference and working electrodes composed of lithium. The scan speed applied for all CV tests was 5 mV/s. A potential with significant increase in the current density is used as limit for the oxidative stability.

The battery tests were performed on a lithium cell cycler (LICCY, development of KIT, Institute of Data Processing and Electronics) with a maximum current of 10 mA and a voltage range of 0 – 10 V. The cut-off voltage is given in the text. The potentials reported in this paper are that of the positive electrode with respect to the counter electrode. The charging and discharging cycles were conducted with constant current based on the C-rate of the material

used. A detailed description can be found in Ref. [21]. Dynamic viscosity was measured using a Malvern Gemini HR Nano rotational rheometer with 40/1° cone geometry and a gap of 30 µm. These experiments were performed by using a solvent evaporation protecting cover in air. The density of the electrolyte mixtures was obtained by repeated measurement of the mass of 75.0 ± 0.2 µl of an electrolyte mixture at room temperature. $^{7}$Li DOSY-NMR measurements were performed on a Bruker Avance III 500 MHz spectrometer at 298K. A detailed description can be found in Ref. [22].

## Results and discussion

### *1. Electrolyte mixtures*

The aim of the study is to evaluate the usability of ionic liquid – sulfolane based mixtures as electrolytes for Li-ion cells. The mixtures fulfill high requirements regarding safety properties, e.g. very high boiling points of >280°C and flash points of >150 °C [14] which makes them intrinsically safe with respect to fire propagation. The components SL, M-SL, and DMMA-TFSA are therefore chosen because of their excellent properties in terms of safety and electrochemical stability [6, 7, 10, 14, 15, 23]. In Table 1, electrolyte mixtures are listed which are studied in detail in the following sections. The lower melting point of M-SL compared to SL makes it a special candidate as electrolyte solvent due to the fact that the electrolyte mixtures remain liquid at lower temperatures. Thus, M-SL is studied as alternative solvent as a substitute for SL. The mixtures EM-1, EM-2, and EM-3 are chosen to compare the pure sulfolane, 3-methylsulfolane, and the ionic liquid DMMA-TFSA, whereas electrolytes EM-4/EM-5 and EM-6/EM-7 represent mixtures of sulfolane and ionic liquid in two selected ratios (1:1 and 2:1 wt.-% solvent).

Table 1. Composition, density and oxidative stability of electrolyte mixtures and solvents.

| sample | solvent 1 | solvent 2 | ratio (solvent 1 : solvent 2) | conducting salt (c / mol kg$^{-1}$) | additive 1 (c [m.-%]) | additive 2 (c [m.-%]) | $E_{ox}$, Li\|Pt [V] | density (25 ± 2) |
|---|---|---|---|---|---|---|---|---|

| | | | | | | | | |
|---|---|---|---|---|---|---|---|---|
| | | | [wt.-%] | | | | | g cm$^{-3}$ |
| SL | SL | - | - | - | - | - | > 5 V[a] | 1.27 ± 0.02<br>1.261[b] |
| M-SL | M-SL | - | - | - | - | - | > 5 V[a] | 1.18 ± 0.01<br>1.194[b] |
| DMMA | DMMA | - | - | - | - | - | 5.6 ± 0.1 | 1.41 ± 0.01 |
| EM-0 | EC | DMC | 1:1 | $LiPF_6$ (1 mol/l) | - | - | 5.6 ± 0.1 | 1.27 ± 0.03<br>1.28[b] |
| EM-1 | SL | - | - | LiTFSA (1) | VC (5) | HMDS (1) | 4.6 ± 0.1 | 1.40 ± 0.01 |
| EM-2 | M-SL | - | - | LiTFSA (1) | VC (5) | HMDS (1) | 4.5 ± 0.1 | 1.34 ± 0.01 |
| EM-3 | DMMA | - | - | LiTFSA (1) | VC (5) | HMDS (1) | 4.7 ± 0.1 | 1.53 ± 0.01 |
| EM-4 | SL | DMMA | 1:1 | LiTFSA (1) | VC (5) | HMDS (1) | 4.8 ± 0.1 | 1.47 ± 0.05 |
| EM-5 | M-SL | DMMA | 1:1 | LiTFSA (1) | VC (5) | HMDS (1) | 4.8 ± 0.1 | 1.41 ± 0.01 |
| EM-6 | SL | DMMA | 2:1 | LiTFSA (1) | VC (5) | HMDS (1) | 5.0 ± 0.1 | 1.44 ± 0.02 |
| EM-7 | M-SL | DMMA | 2:1 | LiTFSA (1) | VC (5) | HMDS (1) | 4.9 ± 0.1 | 1.39 ± 0.02 |

[a] No significant increase of the current density is observed up to 6 V. [b] Value provided by the supplier.

Selected properties are listed in Tab. 1 for comparison, namely the oxidative stability against platinum as an inert working electrode (section 4) and the density. The data of the oxidation stability measurements confirm a good oxidation resistance up to 4.5 – 5 V, which makes the electrolytes promising candidates for high voltage applications. Principally, the density of the electrolyte mixtures is relatively high based on the ionic liquid DMMA-TFSA and the amount of LiTFSA which is dissolved. Nevertheless, an increase in density of about 0.2 g cm$^{-3}$ is still acceptable in view of electrolyte processability. In this case, the viscosity (section 2) plays a more crucial part in the cell processability and cell performance.

*2. Conductivity and viscosity measurements*

In Fig. 1, the temperature dependency of the viscosity (Fig 1a) and the ionic conductivity (Fig 1b) of the electrolytes are shown. Both figures are depicted in logarithmic-scale because of a better visualization of the values. The viscosity $\eta$ is directly linked to the mobility (diffusion coefficient $D$; section 3) in the Stokes-Einstein correlation $D \sim \eta^{-1}$. Thus, the increase in viscosity by 1 – 1.5 orders of magnitude compared to EM-0 is expected to impair the cell performance significantly. However, the overall ionic conductivity is still in the order of >1

mS $cm^{-1}$ at room temperature. Whereas the conductivity of the reference electrolyte EM-0 features an almost linear behavior within the temperature range of 0 – 80 °C, the values of the electrolytes EM-1 – EM-7 can be best described by a quadratic regression. The strong attraction between the ions and the solvent molecules which is also confirmed in the diffusion measurements (section 3) is supposed to be the reason for this behavior. Thus, a higher temperature will affect the mobility of the ions more considerable. This analysis is supported by the viscosity data, which also reveal a strong dependency of the temperature in a non-linear behavior.

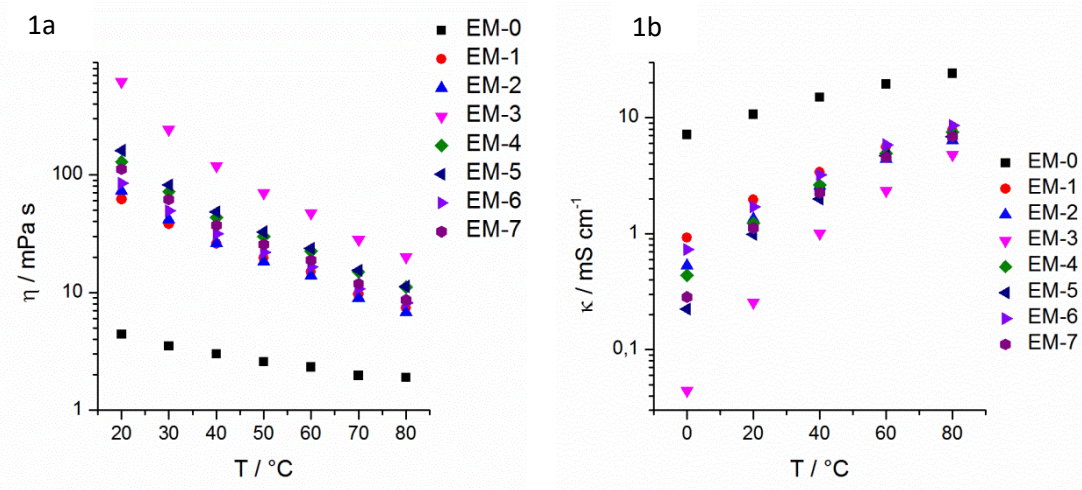


**Figure 1**: Temperature dependent measurement of conductivity (Fig. 1a) and viscosity (Fig. 1b) of the electrolytes EM0 – EM7.

A detailed depiction of the dependence of the conductivity from the DMMA-TFSA/SL wt.-ratio (all samples contain 1 mol $kg^{-1}$ LiTFSA) is shown in Figure 1-SI in the supporting information.

*3. Lithium diffusion and lithium transport numbers*

In Li ion cells, the fast transport of $Li^+$ is one of the most critical points which the electrolyte has to fulfill. Therefore, PFG-NMR (pulsed field gradient NMR) studies are performed to investigate the mobility of the lithium ions in the electrolytes for selected electrolytes.

Exemplarily, the ionic liquid and sulfolane based electrolytes EM-1, EM-3 and EM-4 are measured and compared to an electrolyte mixture widely used today especially by scientific groups (LP30®, EC/DMC + 1M $LiPF_6$) and EC/DMC + 1 mol/kg LiTFSA. The results of the measurements are listed in Tab. 2. The $^1$H-NMR spectra confirm the solvent ratios excellently and do not show any further impurities in the samples (not shown here). The transference numbers are calculated according to $t_i = (\chi_i \cdot D_i)/(\Sigma\, \chi_i \cdot D_i)$ [25] .

Table 2. PFG-NMR results of mixture EM-1, EM-3, and EM-4.

| | EM-0 | EM-1 | EM-3 | EM-4 | E-EC[a] |
|---|---|---|---|---|---|
| $D_{7Li}$ x $10^{-11}$ $m^2$ $s^{-1}$ | 22.4 ± 0.3 | 2.43 ± 0.05 | 0.18 ± 0.01 | 1.15 ± 0.05 | 10.64 ± 0.03 |
| $D_{19F}$ x $10^{-11}$ $m^2$ $s^{-1}$ | 25.3 ± 0.1 | 2.51 ± 0.05 | 0.17 ± 0.05 | 1.05 ± 0.05 | 12.6 ± 0.1 |
| $D_{1H}$ x $10^{-11}$ $m^2$ $s^{-1}$ VC | - | 6.18 ± 0.05 | 0.77 ± 0.05 | 2.90 ± 0.05 | - |
| $D_{1H}$ x $10^{-11}$ $m^2$ $s^{-1}$ $DMMA^+$ | - | | 0.28 ± 0.05 | 1.09 ± 0.05 | - |
| $D_{1H,2}$ x $10^{-11}$ $m^2$ $s^{-1}$ sulfolane | - | 2.51 ± 0.05 | - | 1.19 ± 0.05 | - |
| $D_{1H,}$ x $10^{-11}$ $m^2$ $s^{-1}$ carbonates | 35.64 ± 0.08<br>42.5 ± 0.6 | - | - | - | 18.9 ± 0.1<br>24.8 ± 0.1 |
| $t_{Li}^+$ | 0.47 ± 0.01 | 0.49 ± 0.02 | 0.17 ± 0.05 | 0.30 ± 0.03 | 0.46 ± 0.01 |
| $t_{F}^-$ | 0.53 ± 0.01 | 0.51 ± 0.02 | 0.41 ± 0.12 | 0.48 ± 0.02 | 0.54 ± 0.01 |
| $t_{DMMA}^+$ | - | - | 0.41 ± 0.13 | 0.22 ± 0.03 | - |
| $\kappa$ / mS/cm at 25 °C | 11,1 | 2,24 | 0,363 | 1,5 | 6,85 |
| $\chi$ ($Li^+$) | 0,5 | 0,5 | 0,395 | 0,5663 | 0,5 |
| $\chi$ ($DMMA^+$) | - | - | 0,6050 | 0,4337 | - |
| $\chi$ ($TFSA^-$) | 0,5 ($PF_6^-$) | 0,5 | 1 | 1 | 0,5 |
| $t_{Li+}$ (NMR/AC-IMP) | 0,758 | 0,571 | 0,285 | 0,423 | 0,799 |

[a] Mixture of LiTFSA (1 mol $kg^{-1}$) in EC/DMC (1:1 wt.-%) for comparison; ionic liquid free, additive free

The values of *D* and *t* which are measured for EM-0, are in excellent agreement with literature results for carbonate systems [26]. Li-ions exhibit a diffusion constant of $10.6 \cdot 10^{-11}$ $m^2$ $s^{-1}$ in an organic solvent mixture based on EC and DMC (mixture is comparable to LP-30, but with LiTFSA as conducting salt). In contrast, the mobility of $Li^+$ in mixture EM-1, EM-3, and EM-4 is significantly reduced. The strongest attenuation of the $Li^+$ diffusion constant (one order of magnitude) is observed in mixture EM-3 (pure ionic liquid solvent). It is shown that the diffusion is decelerated in the $^{19}$F and $^1$H spectra as well. This can be related to the strong interaction between the $DMMA^+$ cation, $Li^+$, and the conducting salt anion $TFSA^-$. Thus, the formation of a cluster-like structure $DMMA[Li(TFSA)_2]$ which is pronounced in literature[27-31] in $TFSA^-$ containing ionic liquid mixtures or pure ionic liquids as well, is

supported here. The transference number of $t_{Li}$ = 0.17 in electrolyte EM-3 is relatively high compared to literature results (0.03 for $Li^+$ in LiTFSA/$PYR_{14}$TFSA [25] or 0.02 for $Li^+$ in LiTFSA/MPI-TFSA [32]). In this study, the organic compounds VC and HMDS are also present in the mixtures which results in a weakening of the Li-TFSA-$DMMA^+$ complexes and therefore result in higher lithium mobility. Pure SL (relative permittivity $\varepsilon_v$ = 43.4 (50 Hz); dipole moment $\mu$ = 4.7 debye[33]) reduces the diffusion constant of $Li^+$, $TFSA^-$ and the $^1$H-signal of SL compared to sample E-EC (EC: $\varepsilon_v$ = 89.8 (at 313 K)[34], $\mu$ = 4.87[35]; DMC: $\varepsilon_v$ = 3.1[34], $\mu$ = 0.91[36]). This can be attributed to the enhanced dipole moment of SL compared to the EC/DMC-mixture (1:1 wt.-%) and the higher viscosity of sample EM-1 ($\eta$ = 62.0 mPa·s) compared to E-EC ($\eta$ = 8.4 mPa·s). Thus, an increased interaction can be inferred between SL and Li-TFSA compared to EC/DMC and Li-TFSA. In EM-4, the mobility of $^7$Li, $^{19}$F, and $^1$H is significantly enhanced compared to mixture EM-3. Indeed, the diffusion constants are in the same order of magnitude when compared to the pure SL mixture EM-1. This implies that SL considerably impedes the formation of $DMMA_{n-1}[Li(TFSA)_n]$ complexes. VC is used in the mixtures because of the necessity as SEI forming agent at the

negative electrode side (graphite) in ionic liquid mixtures. However, it is seen that it affects the cluster structure and formation only slightly. Summarizing, a significant reduction of the $Li^+$ mobility is observed in SL and SL+DMMA-TFSA electrolytes compared to organic carbonates (EC/DMC) which will influence the cell performance in Li-ion batteries.

The transference numbers can be calculated in a different manner taking account of the Nernst-Einstein equation and the ionic conductivity [22]. In table 3, the values which are calculated according to the quotient $\sigma_{Li}$ / $\sigma_{impedance}$ are mentioned as $t_{Li+}$ (NMR/AC-IMP) in Tab. 2. Principally, the partial Li conductivity $\sigma_{Li}$ can be calculated via the Nernst-Einstein equation

$$D_{\mathrm{Li}} = H_{\mathrm{R}} \cdot \frac{\sigma_{\mathrm{Li}} \cdot k_{\mathrm{B}} \cdot T}{N_{\mathrm{Li}} \cdot q_{\mathrm{Li}}^2}$$

where $k_B$ is the Boltzmann constant, $T$ the temperature, $N_{Li}$ the number density of Li ions and $q_{Li}$ their charge. $H_R$ is the Haven ratio which is equal to one for uncorrelated motion of the charge carriers (used for the calculations). It is seen that the values calculated on the basis of the partial lithium conductivity $\sigma_{Li}$ overestimate the lithium mobility significantly which is a result of a Haven ratio which is not equal to 1 for real concentrated electrolyte systems [37]. However, the values can be seen as an upper limit of the transference number.

*4. Oxidative stability of the electrolytes*

As shown in Tab. 1, an excellent oxidative stability against platinum is observed for the electrolyte mixtures. The detailed behavior of the current density response is depicted in figure 2. Here, the oxidation stability $E_{ox}$ against Pt (three electrode configuration) is proven to be >4.5 V vs. $Li/Li^+$ for the electrolytes. Although the electrodes lithium and platinum cannot be compared directly to cell electrodes (graphite, NMC, $LiCoPO_4$), a high oxidative stability of the electrolytes is still observed. Thus, the oxidative stabilities of the electrolytes should be suitable in real cell configurations up to 4.2 – 4.5 V vs. $Li/Li^+$. The values are comparable to those published by Xiang et al. for piperidinium based IL – SL mixtures and LiTFSA [20]. It can be seen, that for the $PP_{14}$-TFSI/SL mixture a slight increase in the current density $j$ starts around 4.5 V, which is in good agreement to the findings here for ammonium based IL-SL mixtures [20].

2a 2b

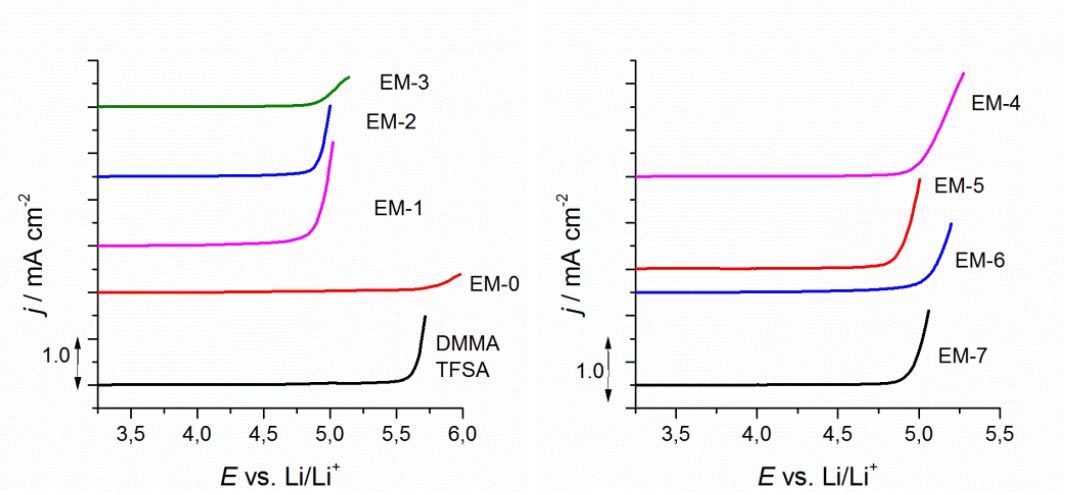


**Figure 2**: CV diagrams of selected electrolyte mixtures. Fig 2a: Mixtures EM0 – EM3; Fig. 2b: Mixtures EM4 – EM7. The second scan from 3.25 to 6 V (5 mV $s^{-1}$) is depicted in comparison.

Additionally, the oxidative stability against aluminum is investigated in Li|Al cells in chronoamperometry measurements (Fig. 3). The time was set to 48h because it is already described that an increase of the current density response which can be attributed to aluminum dissolution can arise after several hours (6 h) retarded based on slow destruction of the passivation layer and electrolyte oxidation [19, 38]. It can be seen, that the reference electrolyte EM-0 exhibits extraordinary stability based on the conducting salt $LiPF_6$. However, a decrease of the current density response is also observed in case of LiTFSA as conducting salt. After a slight increase at the beginning of the polarization, a decrease within 6-10 h is observed. It can be deduced that the aluminum dissolution is hampered in all cases. The hindrance of the dissolution of Al complexes which is said to be the cause for a better Al stability can be a main reason in the novel electrolytes. The results confirm the findings of enhanced stability (oxidative resistance) of sulfolanes and LiTFSA when ionic liquids are added as solvents to the electrolytes [39].

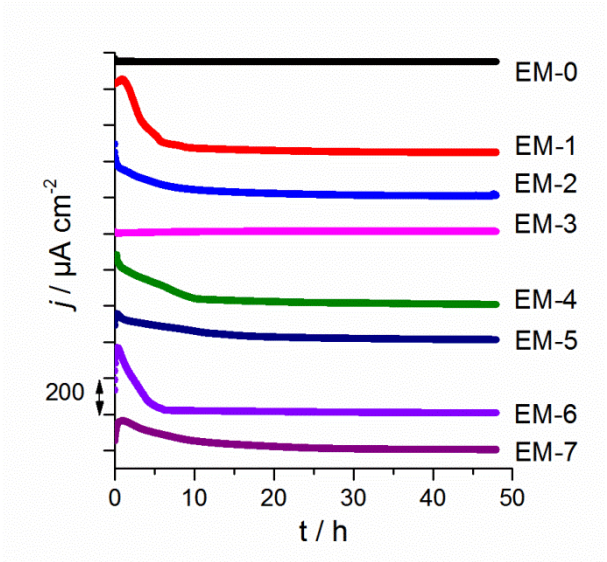


**Figure 3**: Chronoamperograms at 4.4 V vs. Li/Li$^+$ of Li|Al cells (Swagelok configuration) at room temperature.

*5. Cell cycling tests (graphite - NMC) of sulfolane and DMMA-TFSA based electrolytes*

The cell performances of the electrolytes EM-1, EM-2, and EM-3 in NMC|C cells are depicted in Figure 1a for 100 cycles. The electrolyte formulations EM-4, EM-5, EM-6, and EM-7 are shown in Figure 1b for comparison. Principally, one cell is shown for each mixture, but in repeated experiments it is demonstrated, that different cells which contain the same electrolyte mixture perform in a comparable manner. It can be seen, that the pure ionic liquid DMMA-TFSA as solvent (mixture EM-3) is not able to achieve an acceptable cell performance even at low C-rates. This is a consequence of the high viscosity of pure ionic liquid mixtures and in particular of the low Li diffusion, mentioned in Table 3. In contrast, electrolyte EM-1 exhibits a cycling performance of ~115 mAh g$^{-1}$ at C/5, which is ~81% of the capacity obtained by electrolyte EM-0 (LP30®, ~142 mAh g$^{-1}$ at C/5, not shown here) as a consequence of the reduced Li$^+$ diffusion constant and higher viscosities (see Table 2 and 3). By comparing sulfolane (SL) and 3-methylsulfolane (M-SL) it is found that the performance of M-SL is significantly reduced. Principally, the melting point of M-SL is lower than that of SL (M-SL: mp = 1 °C;. SL: mp = 27.5 °C) because of the steric hindrance of the additional methyl group which prevents the formation of a crystal lattice. Thus, M-SL can be used at

lower temperatures. However, if the mixture is in the liquid phase, SL yields the better performance on account of a reduced viscosity and higher ionic conductivity compared to M-SL mixtures.

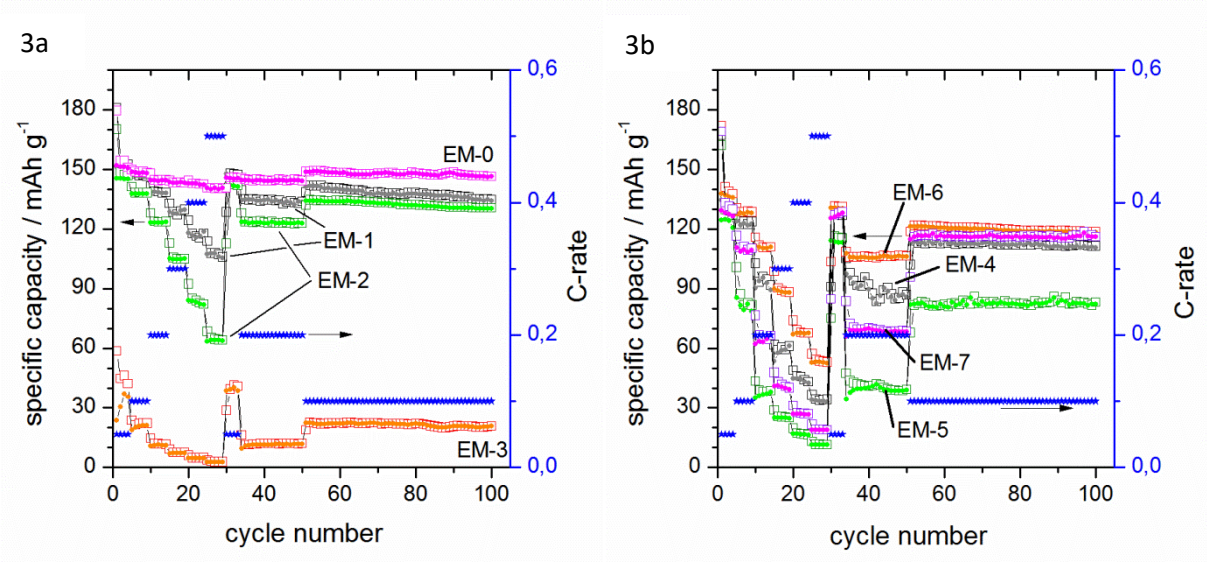


**Figure 4**: Charge and discharge capacity of mixture EM-*n* (Fig. 1a: *n* = 1-3; Fig 1b: *n* = 4-7). Cell configuration: C|NMC. square = charging, circle = discharging. The variation of coin cell tests with the same electrolyte mixture is in the order of ±6 mAh $g^{-1}$.

The mobility of $Li^+$ is slightly hindered compared to electrolyte EM-0 (EC/DMC). This can be also observed by comparing the initial internal resistance. In case of E-0 (EC/DMC), the internal resistance is 4.5 ± 1 Ω (coin cell) after the assembling of the cell (before the cycling, $U_o$ ~ 0.3 V). The electrolytes EM-1, EM-2, and EM-3 result in internal resistances of 15.6 ± 2 Ω (EM-1), 21.4 ± 3 Ω (EM-2), 56.5 ± 5 Ω (EM-3), before the cycling is started. The differences in the internal resistance are caused by the different electrolyte solvents. The detailed efficiencies of the cells regarding the specific capacity at a defined C-rate are listed in Table 1-SI (supporting information). It is observed that both solvents can be successfully used as electrolytes with DMMA-TFSA as co-solvent in 1:1 and 2:1 wt.-ratio (SL-component:

DMMA-TFSA) with a significant increase of the specific capacity at 2:1 wt.-ratios. Principally it is possible to achieve higher capacity values in mixtures containing SL instead of M-SL at the same C-rate. At C/5, this behavior can be seen distinctly (at cycles 35 – 50). The better performance of SL-electrolytes can be assigned to the higher viscosity of M-SL compared to SL. Consequently, the conductivities of the SL+DMMA-TFSA mixtures are higher compared to the equivalent M-SL mixtures (compare Table 2, section 2). Thus, the limiting factor regarding to the capacity values is considered to be the mobility of the $Li^+$ ions. Here it is assumed that the mobility of the Li-ions in the M-SL mixture is impeded because of the steric hindrance of the additional methyl group. Because of the similar chemical environment at the polar centers and composition of the electrolytes, the formation of Li-clusters (e.g. $LiTFSA_n^{-(n-1)}$) is assumed to be similar for both solvents (SL and M-SL).

Table 3. Internal resistance and cell voltage of stored Li-ion cells which are charged to 3.8 V (0.05 C, RT, constant current only)

| | | after 100 cycles | after charging to 3.8 V (CC charging) | after 1 month staying | | after 2 month staying | | after 8 month staying | |
|---|---|---|---|---|---|---|---|---|---|
| **EM-6** | *E* / V | 3.185 | 3.759 | 3.743 | -0.43% | 3.731 | -0.74% | 3.675 | -2.25% |
| | *R* / Ω | 24.7 | 25.45 | 23.46 | | 26.32 | | 25.9 | |

At room temperature (25 ± 2°C ), the energy efficiency of the NMC|C cell by using the solvent sulfolane (EM-1) is ≥ 90% up to C/5, whereas the extractable capacity declines to 73% (113 mAh $g^{-1}$). In electrolyte mixture EM-4, the decrease of the specific capacity at increasing C-rates is even more pronounced. However, the resistance against corrosion is significantly improved in case of electrolyte EM-4 [14]. Principally, the use of electrolytes which are not able to deliver an acceptable mobility of $Li^+$ ions is restricted. On the other side, a significant improvement of safety and stability can be reached [40].

Figure 2a illustrates the specific capacity as a function of the C-rate for electrolyte EM-4. In Figure 2b, the voltage response of the NMC|C cell (electrolyte EM-4) is depicted versus charging time. Principally, NMC is set as the limiting electrode, thus enough graphite is

available inside the cell for intercalation of lithium. The voltage limit for fully extracting all lithium from NMC (1 equivalent Li, theoretical capacity of NMC = 277.85 mAh $g^{-1}$) is ~4.8 V which is in good agreement to the NMC characteristics studied by Yabuuchi at al.[41]. Thereafter, a rapid increase in voltage is observed. In addition, the figure reveals that the electrolyte is stable up to at least 4.8 V with NMC and C electrodes because the whole current is used for extracting lithium out of NMC. The high voltage stability is a second favor which makes the electrolyte formulation interesting for high voltage studies and applications. Because of the most balanced properties in efficiency, cycle-ability, aluminum corrosion [14], and safety, the electrolytes EM-4 and EM-6 are studied in more detail in the following sections regarding additives and temperature dependence.

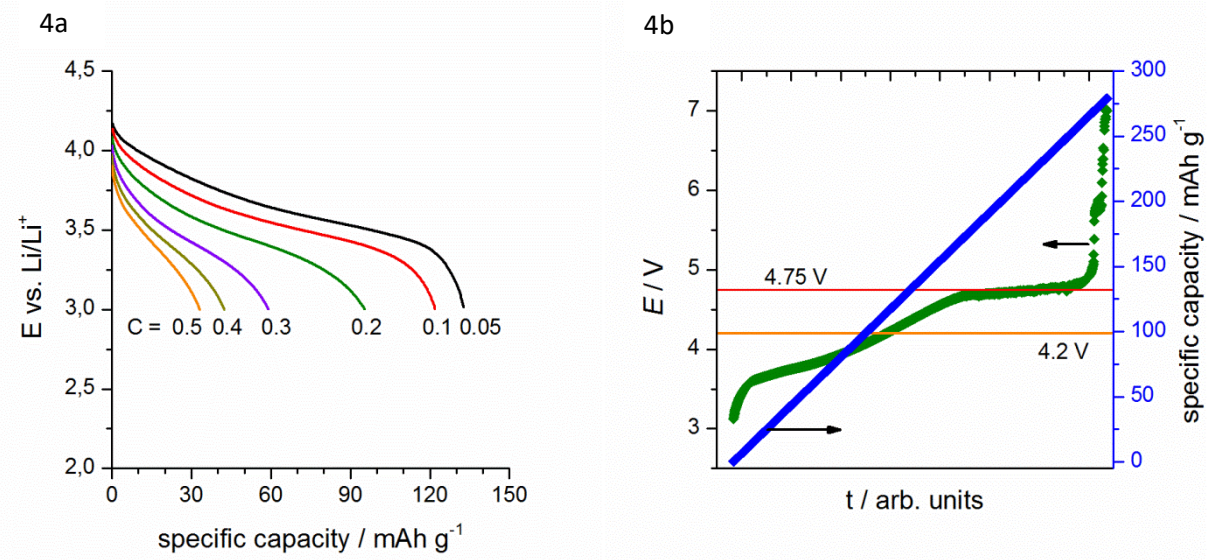


**Figure 5**: Fig. 2a: Cell voltage as a function of the discharge capacity of mixture EM-4 at RT in C|NMC cell configuration. Fig. 2b: Cell voltage and specific capacity of electrolyte EM-4 in C|NMC cell configuration at RT (C/10) by overcharging.

*5. Temperature dependence of cell cycling tests*

The cell performance of two selected mixtures is studied for different temperatures. Here, EM-1 and EM-4 are chosen based on performance effects at room temperature and the temperature effects of ionic liquid containing electrolytes. In Figure 3, the specific capacity of

NMC|C cells with electrolyte EM-1 are depicted at different temperatures starting from the 11$^{nd}$ cycle, namely 20 °C, 30 °C, 40 °C, and 50 °C (same temperature for charging and discharging). During the first 10 cycles, the cell formation is performed successfully at 25 °C. Here, all cells exhibit a similar initial capacity at RT. It can be clearly seen, that the most significant effect can be observed between 30 °C and 40 °C. Higher temperatures have only a small impact on the C-rates (up to 1C).

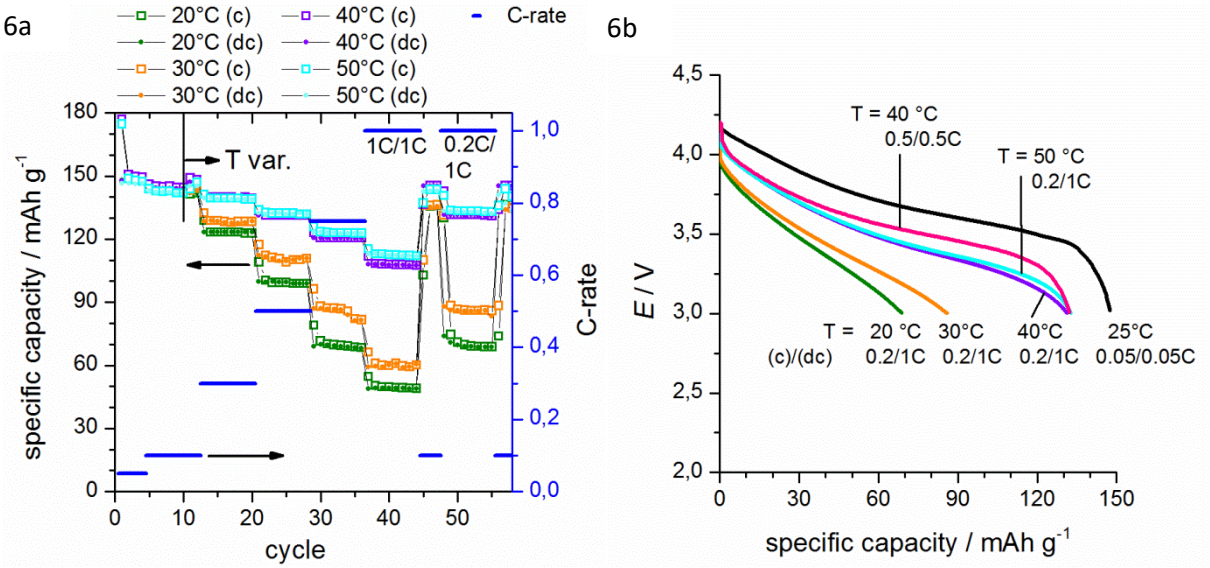


**Figure 6**: Temperature dependence of the specific capacity of electrolyte EM-1. Figure 3a: Effect of temperature after the formation at RT within the first 10 cycles. Figure 3b: Discharge profile at C/20 (RT, 3$^{rd}$ cycle) and at 0.2C/1C (53. cycle) at different temperatures. Cell configuration: C|NMC. (c) = charging, (dc) = discharging. The variation of coin cell tests with the same electrolyte mixture is in the order of ±6 mAh g$^{-1}$.

However, it is possible to increase the accessible specific capacity by a factor of 2.7 if the temperature is slightly elevated to 40 °C and the charging is performed at low C-rates (C/5). In this case, even at 1C a discharge capacity of >130 mAh g$^{-1}$ can be achieved with the mixture EM-1. In Figure 3b, the discharge profiles are depicted at selected C-rates. For comparison, the discharge at C/20 at the beginning (3$^{rd}$ cycle) and at C/2 (cycle 26, 40 °C) are depicted as well. It can be seen that the voltage of the plateau is reduced in case of higher C-

rates compared to C/20. Nevertheless, the energy efficiency at 40°C is still >90% (93.7% @ C/2 and 91.6% @ 1C; 98.0% @ C/10 in cycle 58).

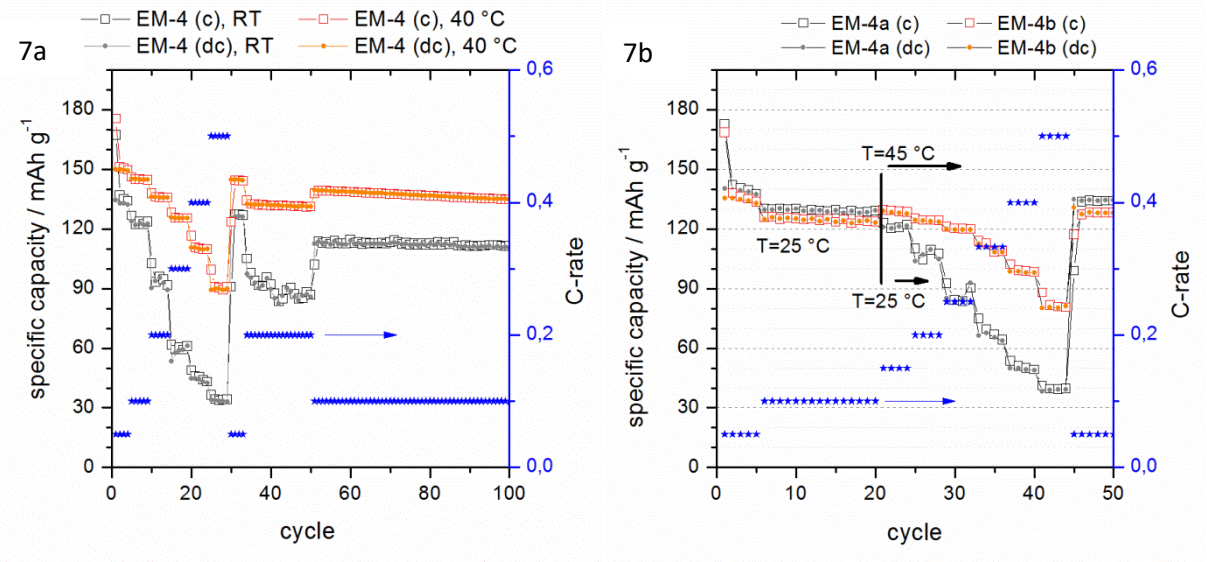


**Figure 7**: Temperature dependence of the specific capacity of electrolyte EM-4. Figure 4a: Comparison of two identical cells at different temperature. Figure 4b: Effect of temperature after the formation at RT. Cell configuration: C|NMC.

The change of the performance of electrolyte EM-4 with increasing temperature is investigated at slightly elevated temperatures (40 °C and 45 °C), too. In Figure 4a, both temperatures (25 ± 3 °C and 40 ± 1 °C) are compared in C|NMC cell configuration. It can be seen that the drop in the specific capacity is reduced significantly at elevated temperatures and a stable cycling with capacities of >130 mAh $g^{-1}$ can be obtained at C/5. However, the cycling stability deteriorates if the formation of the cell (growing of the SEI layer) is also performed at elevated temperatures. In Figure 4b, two identical cells are depicted which are cycled at room temperature (25 ± 2 °C) for 20 cycles. Thereafter, one cell is cycled at 45 °C (EM-4b) and the other cell at RT. It can be observed that at moderate C-rates (C/5, C/4) the specific capacity at 45 °C is still > 120 mAh $g^{-1}$, whereas an anticlimax can be seen at RT (EM-4a, 80 – 90 mAh $g^{-1}$ at C/4). This corroborates the severe temperature dependence of the viscosity, conductivity and $Li^+$ diffusion in this temperature range. At slow C-rates (C/20), a comparable

performance is found for both temperatures. The experiments demonstrate that small changes in temperature of $\Delta$ = 10 – 20 °C result in significant effects on the cycling performance of the cells. This means that even small increases in temperature allows for cycling the cells with acceptable cell performances, even applying ionic liquids. Conversely, the experiments also reveal that a decrease in temperature can cause as significant reduction of the accessible power of a cell performed with the electrolytes mentioned.

~~6. Cell cycling tests in dependence of various VC and HMDS concentrations~~

~~7. Effect of LiBOB in sulfolane and methylsulfolane containing electrolytes~~

## Conclusion

In this study novel electrolyte formulations based on sulfolane, 3-methylsulfolane, LiTFSA, and the ionic liquid DMMA-TFSA are prepared and examined in NMC|C lithium ion cells. For the first time, these mixtures are studied against graphite electrodes which are the most common type of negative electrodes in Li-ion cells today. The electrolyte components are chosen because of their high flash points which makes them intrinsically safe with respect to fire propagation. Vinylene carbonate (VC) and hexamethyldisilazane (HMDS) are used as additives for improving the cell performance. It is demonstrated that the electrolytes exhibit a wide electrochemical window ( up to 4.7 V) and excellent compatibilities with NMC and C electrodes. Further it is shown that by rising the temperature slightly a significant improvement of the cell performance can be obtained.

## 5. Acknowledgements

AH acknowledges support by Deutsche Forschungsgemeinschaft (Sachbeihilfe, HO 5266/1-1). We acknowledge IoLiTec Ionic Liquids Technologies GmbH for kindly providing the ionic liquid DMMA-TFSA and Chemetall for providing lithium bis(oxalato)borate. We thank

Martin Tosoni for helpful discussions. We thank Matthias Migeot and Ceylan Yildiz for performing selected electrochemical measurements.

## References

[1] S.-P.S. Yen, B.J. Carter, D.H. Shen, R.B. Somoano, High cycle life secondary lithium battery, in: C.I.o. Technology (Ed.)United States, 1985.
[2] K. Xu, C.A. Angell, High Anodic Stability of a New Electrolyte Solvent: Unsymmetric Noncyclic Aliphatic Sulfone, J. Electrochem. Soc., 145 (1998) L70-L72.
[3] X.-G. Sun, C.A. Angell, New sulfone electrolytes for rechargeable lithium batteries, Electrochem. Commun., 7 (2005) 261-266.
[4] Y. Matsuda, M. Morita, K. Yamada, K. Hirai, Characteristics of Sulfolane-Based Electrolytes for Rechargeable Lithium Batteries, J. Electrochem. Soc., 132 (1985) 2538-2543.
[5] V.S. Kolosnitsyn, L.V. Sheina, S.E. Mochalov, Physicochemical and electrochemical properties of sulfolane solutions of lithium salts, Russ. J. Electrochem. , 44 (2008) 575-578.
[6] M. Sedlarikova, J. Vondrak, J. Maca, K. Bartusek, Sulfolane as Solvent for Lithium Battery Electrolytes, J. New Mat. Electrochem. Systems, 2 (2013) 065-071
[7] C. Nanjundiah, J.L. Goldman, L.A. Dominey, V.R. Koch, Electrochemical Stability of LiMF[sub 6] (M = P, As, Sb) in Tetrahydrofuran and Sulfolane, J. Electrochem. Soc., 135 (1988) 2914-2917.
[8] A. Abouimrane, I. Belharouak, K. Amine, Sulfone-based electrolytes for high-voltage Li-ion batteries, Electrochem. Commun., 11 (2009) 1073-1076.
[9] K. Xu, C.A. Angell, Sulfone-Based Electrolytes for Lithium-Ion Batteries, J. Electrochem. Soc., 149 (2002) A920.
[10] S. Li, B. Li, X. Xu, X. Shi, Y. Zhao, L. Mao, X. Cui, Electrochemical performances of two kinds of electrolytes based on lithium bis(oxalate)borate and sulfolane for advanced lithium ion batteries, J. Power Sources, 209 (2012) 295-300.
[11] H. Nakagawa, Y. Fujino, S. Kozono, Y. Katayama, T. Nukuda, H. Sakaebe, H. Matsumoto, K. Tatsumi, Application of nonflammable electrolyte with room temperature ionic liquids (RTILs) for lithium-ion cells, J. Power Sources, 174 (2007) 1021-1026.
[12] H. Nakagawa, S. Izuchi, K. Kuwana, T. Nukuda, Y. Aihara, Liquid and Polymer Gel Electrolytes for Lithium Batteries Composed of Room-Temperature Molten Salt Doped by Lithium Salt, J. Electrochem. Soc., 150 (2003) A695.
[13] H. Sakaebe, H. Matsumoto, N-Methyl-N-propylpiperidinium bis(trifluoromethanesulfonyl)imide (PP13-TFSI) - novel electrolyte base for Li battery, Electrochem. Commun., 5 (2003) 594-598.
[14] A. Hofmann, L. Merklein, M. Schulz, T. Hanemann, Anodic Aluminum Dissolution of LiTFSA Containing Electrolytes for Li-Ion-Batteries, Electrochim. Acta, (2013).
[15] T. Sato, T. Maruo, S. Marukane, K. Takagi, Ionic liquids containing carbonate solvent as electrolytes for lithium ion cells, J. Power Sources, 138 (2004) 253-261.
[16] S. Seki, Y. Ohno, H. Miyashiro, Y. Kobayashi, A. Usami, Y. Mita, N. Terada, K. Hayamizu, S. Tsuzuki, M. Watanabe, Quaternary Ammonium Room-Temperature Ionic Liquid/Lithium Salt Binary Electrolytes: Electrochemical Study, J. Electrochem. Soc., 155 (2008) A421-A427.
[17] K. Xu, S. Zhang, T.R. Jow, W. Xu, C.A. Angell, LiBOB as Salt for Lithium-Ion Batteries:A Possible Solution for High Temperature Operation, Electrochem. Solid-State Lett., 5 (2002) A26-A29.
[18] M. Dahbi, F. Ghamouss, F. Tran-Van, D. Lemordant, M. Anouti, Comparative study of EC/DMC LiTFSI and LiPF6 electrolytes for electrochemical storage, J. Power Sources, 196 (2011) 9743-9750.
[19] R.-S. Kühnel, M. Lübke, M. Winter, S. Passerini, A. Balducci, Suppression of aluminum current collector corrosion in ionic liquid containing electrolytes, J. Power Sources, 214 (2012) 178-184.
[20] J. Xiang, F. Wu, R. Chen, L. Li, H. Yu, High voltage and safe electrolytes based on ionic liquid and sulfone for lithium-ion batteries, J Power Sources, 233 (2013) 115-120.

[21] A. Hofmann, M. Schulz, T. Hanemann, Effect of Conducting Salts in Ionic Liquid based Electrolytes: Viscosity, Conductivity, and Li-Ion Cell Testing, Int. J. Electrochem. Sci., 8 (2013) 10170-10189.
[22] S. Indris, R. Heinzmann, M. Schulz, A. Hofmann, Ionic Liquid Based Electrolytes: Correlating Li Diffusion Coefficients and Battery Performance, submitted, (2014).
[23] A. Lewandowski, B. Kurc, I. Stepniak, A. Swiderska-Mocek, Properties of Li-graphite and LiFePO4 electrodes in LiPF6–sulfolane electrolyte, Electrochim. Acta, 56 (2011) 5972-5978.
[24] H. Xie, Z. Tang, Z. Li, Y. He, H. Wang, Y. Liu, Aluminum Corrosion Behavior of LiBOB in Composite Polymer Electrolyte for Li-Polymer Batteries, Electrochem. Solid-State Lett., 11 (2008) C19-C22.
[25] F. Castiglione, R. Enzio, M. Andrea, P. Stefano, Molecular Environment and Enhanced Diffusivity of Li+ Ions in Lithium-Salt-Doped Ionic Liquid Electrolytes, J. Phys. Chem. Lett., 2 (2011) 153–157.
[26] Handbook of Battery Materials, 2. ed., WILEY-VCH, Weinheirn, 2011.
[27] A. Shirai, K. Fujii, S. Seki, Y. Umebayashi, S.-i. Ishiguro, Y. Ikeda, Solvation of Lithium Ion in N,N-Diethyl-N-methyl-N-(2-methoxyethyl)ammonium Bis(trifluoromethanesulfonyl)-amide Using Raman and Multinuclear NMR Spectroscopy, Anal. Sci., 24 (2008) 1291-1296.
[28] S. Duluard, J. Grondin, J.-L. Bruneel, I. Pianet, A. Grélard, G. Campet, M.-H. Delville, J.-C. Lassègues, Lithium solvation and diffusion in the 1-butyl-3-methylimidazolium bis(trifluoromethanesulfonyl)imide ionic liquid, J. Raman Spectros., 39 (2008) 627-632.
[29] J.-C. Lassègues, J. Grondin, D. Talaga, Lithium solvation in bis(trifluoromethanesulfonyl)imide-based ionic liquids, Phys. Chem. Chem. Phys., 8 (2006) 5629.
[30] Y. Saito, T. Umecky, J. Niwa, T. Sakai, S. Maeda, Existing Condition and Migration Property of Ions in Lithium Electrolytes with Ionic Liquid Solvent, J. Phys. Chem. B, 111 (2007) 11794-11802.
[31] T. Umecky, Y. Saito, Y. Okumura, S. Maeda, T. Sakai, Ionization Condition of Lithium Ionic Liquid Electrolytes under the Solvation Effect of Liquid and Solid Solvents, J. Phys. Chem. B, 112 (2008) 3357-3364.
[32] T.-Y. Wu, L. Hao, P.-R. Chen, J.-W. Liao, Ionic Conductivity and Transporting Properties in LiTFSI-Doped Bis(trifluoromethanesulfonyl)imide-Based Ionic Liquid Electrolyte Int. J. Electrochem. Sci., 8 (2013) 2606 - 2624.
[33] C. Liang, F. Wang, Y. Xu, J. Chen, D. Liu, Z. Luo, A stable electrolyte makes a nonaqueous Li–O2 battery truly rechargeable, New J. Chem. , 37 (2013) 2568.
[34] M. Morita, Y. Asai, N. Yoshimoto, M. Ishikawa, A Raman spectroscopic study of organic electrolyte solutions based on binary solvent systems of ethylene carbonate with low viscosity solvents which dissolve different lithium salts, J. Chem. Soc., Faraday Trans., 94 (1998) 3451-3456.
[35] R.P. Seward, E.C. Vieira, The Dielectric Constants of Ethylene Carbonate and of Solutions of Ethylene Carbonate in Water, Methanol, Benzene and Propylene Carbonate, J. Phys. Chem. B, 62 (1958) 127-128.
[36] P. Tundo, M. Selva, The Chemistry of Dimethyl Carbonate, Acc. Chem. Res., 35 (2002) 706-716.
[37] S. Zugmann, Messung von Lithium-Ionen Überführungszahlen an Elektrolyten für Lithium-Ionen Batterien, Universität Regensburg, Regensburg, 2011.
[38] E. Krämer, T. Schedlbauer, B. Hoffmann, L. Terborg, S. Nowak, H.J. Gores, S. Passerini, M. Winter, Mechanism of Anodic Dissolution of the Aluminum Current Collector in 1 M LiTFSI EC:DEC 3:7 in Rechargeable Lithium Batteries, J. Electrochem. Soc., 160 (2012) A356-A360.
[39] A. Hofmann, L. Merklein, M. Schulz, T. Hanemann, Anodic Aluminum Dissolution of LiTFSA Containing Electrolytes for Li-Ion-Batteries, Electrochim. Acta, 116 (2014) 388-395.
[40] B. Scrosati, J. Garche, Lithium batteries: Status, prospects and future, J. Power Sources, 195 (2010) 2419-2430.
[41] N. Yabuuchi, Y. Makimura, T. Ohzuku, Solid-State Chemistry and Electrochemistry of LiCo[sub 1/3]Ni[sub 1/3]Mn[sub 1/3]O[sub 2] for Advanced Lithium-Ion Batteries, J. Electrochem. Soc., 154 (2007) A314-A321.

## List of Tables

**List of Figure captions**

## List of Figures

# Supporting Information

## Ionic Liquid Based High Temperature and High Voltage stable Electrolytes for Li-ion batteries

Andreas Hofmann, Michael Schulz, Ralf Heinzmann, Sylvio Indris, Thomas Hanemann

### 1. Conductivity measurements

The dependency of the system LiTFSA (1 mol $kg^{-1}$) in DMMA-TFSA + SL electrolyte solvent (without additional additives) is depicted in Figure 1-SI.

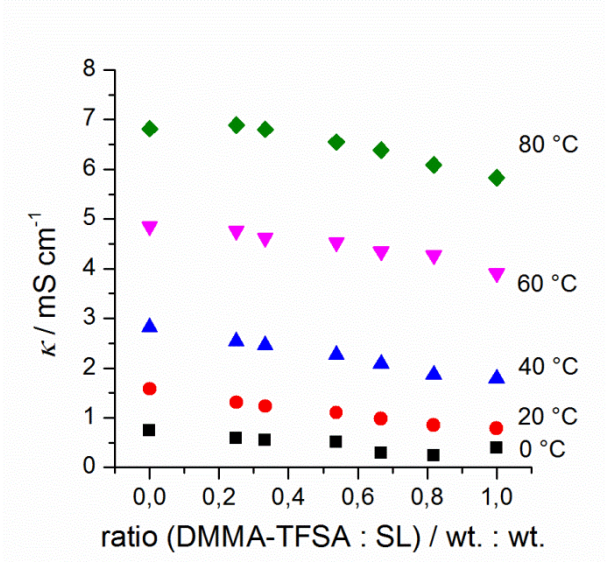


**Figure 1-SI**: Temperature dependency of DMMA-TFSA + SL + LiTFSA (1 mol $kg^{-1}$) mixtures (wt./wt.-ratio of the solvent system).

### 2. Cycling results of the cells

The Coulomb efficiency mentions the percentage of energy, which can be retained from the energy which is used for the charging of the battery cell.

| **Table 1-SI**. Energy data of the NMC\|C cells performed by using electrolyte E-1, E-2, and E-3. | | | | | | | | | |
|---|---|---|---|---|---|---|---|---|---|
| cycle | | 6 | 12 | 18 | 24 | 29 | 50 | 52 | 100 |
| C-rate[a] | | 0.1 | 0.2 | 0.3 | 0.4 | 0.5 | 0.2 | 0.1 | 0.1 |
| EM-0 | discharge capacity mAh $g^{-1}$ | 148.0 | 144.6 | 142.4 | - | 140.0 | - | 146.4 | 144.8 |
| | energy efficiency[b] / % | 98.2 | 97.4 | 96.4 | - | 95.7 | - | 98.8 | 98.1 |
| | percent initial (6. cycle) capacity at 0.1C | 100 | 97.7 | 96.2 | - | 95.0 | - | 98.9 | 97.8 |
| EM-1 | discharge capacity mAh $g^{-1}$ | 154.7 | 146.3 | 137.3 | 126.4 | 113.3 | 141.5 | 149.5 | 142.7 |
| | energy efficiency / % | 96.5 | 94.9 | 93.5 | 92.4 | 89.9 | 94.7 | 96.8 | 96.5 |
| | percent initial (6. cycle) capacity at 0.1C | 100 | 94.6 | 88.8 | 81.8 | 73.2 | 91.5 | 96.7 | 92.2 |
| EM-2 | discharge capacity mAh $g^{-1}$ | 137.8 | 123.2 | 104.6 | 82.2 | 64.0 | 123.6 | 134.0 | 130.2 |
| | energy efficiency / % | 94.6 | 91.5 | 88.5 | 86.3 | 85.2 | 91.9 | 95.2 | 95.1 |
| | percent initial (6. cycle) capacity at 0.1C | 100 | 89.5 | 75.9 | 59.7 | 46.5 | 89.7 | 97.3 | 94.5 |
| EM-3 | discharge capacity mAh $g^{-1}$ | 21.7 | 12.3 | 7.9 | 5.0 | 3.1 | 12.7 | 24.1 | 22.6 |
| | energy efficiency / % | 84.0 | 83.2 | 81.6 | 79.8 | 78.7 | 85.7 | 89.4 | 90.9 |
| | percent initial (6. cycle) capacity at 0.1C | 100 | 56.7 | 36.3 | 23.3 | 14.2 | 58.8 | 111.3 | 104.4 |
| EM-4 | discharge capacity mAh $g^{-1}$ | 121.9 | 95.4 | 59.1 | 42.4 | 33.5 | 85.6 | 113.4 | 110.6 |
| | energy efficiency / % | 92.9 | 89.1 | 87.9 | 86.3 | 83.9 | 88.4 | 93.7 | 93.2 |
| | percent initial (6. cycle) capacity at 0.1C | 100 | 78.3 | 48.5 | 34.8 | 27.2 | 70.2 | 93.0 | 90.8 |
| EM-5 | discharge capacity mAh $g^{-1}$ | 81.4 | 37.1 | 25.0 | 16.6 | 11.4 | 38.6 | 82.7 | 82.5 |
| | energy efficiency / % | 83.2 | 84.0 | 83.8 | 81.9 | 80.9 | 87.4 | 89.2 | 90.2 |
| | percent initial (6. cycle) capacity at 0.1C | 100 | 45.6 | 30.7 | 20.3 | 14.1 | 47.5 | 101.6 | 100.9 |
| EM-6 | discharge capacity mAh $g^{-1}$ | 127.9 | 110.2 | 88.0 | 67.4 | 52.8 | 106.4 | 121.0 | 118.2 |
| | energy efficiency / % | 94.5 | 91.9 | 89.4 | 87.9 | 87.1 | 91.8 | 94.7 | 94.5 |
| | percent initial (6. cycle) capacity at 0.1C | 100 | 86.2 | 68.8 | 52.7 | 41.3 | 83.2 | 94.6 | 92.4 |
| EM-7 | discharge capacity mAh $g^{-1}$ | 108.7 | 63.2 | 39.8 | 26.7 | 18.7 | 68.3 | 116.7 | 116.2 |
| | energy efficiency / % | 89.7 | 85.0 | 83.3 | 82.5 | 80.9 | 86.1 | 91.9 | 92.0 |
| | percent initial (6. cycle) capacity at 0.1C | 100 | 58.1 | 36.6 | 24.5 | 17.2 | 62.8 | 107.3 | 106.9 |

[a] The C-rate of charging and discharging is the same. [b] The energy efficiency is choosen because it considers the charge as well as the voltage.